Electric Screen Jauman Absorber Design Algorithms

Leendert Johannes du Toit, *Member, IEEE*, and Johannes Hendrik Cloete, *Member, IEEE*

***Abstract*—The electric screen Jauman absorber [1] is a stratified cascade of dielectric spacers, interlaced with resistive sheets, which is effective in reducing specular reflection from flat or moderately curved conducting surfaces. A literature survey of the period up to 1993 may be found in [2], while the topic has also received more recent attention, e.g., [3]–[9]. Usually, the dielectric constant of the identical spacers is assumed known *a priori,* and the design problem is to find the sheet surface resistivities that will yield an absorption behavior which meets certain design criteria. This paper presents detail on three efficient and dedicated synthesis algorithms that synthesize absorbers with Butterworth, Equiripple, and Chebyshev absorption properties and should be seen as complementary to the introductory discussion in [2]. To the authors' knowledge, the Chebyshev solutions solve the fundamental problem for the first time.**

I. Introduction

BORROWING FROM the development in [2], the design problem may be related to the network shown in Fig. 1, normalized to the intrinsic impedance of free-space and to a center frequency of 1/4 Hz. The resistive sheets are represented by lumped shunt conductances, $0 < G_i <, \infty i = 1 \cdots N$, related to the sheets by $G_i = \eta_0/R_{s,i} = 1/R_i$, with $\eta_0 = \sqrt{\mu_0/\epsilon_0}$, and $R_{s,i}$ being the various unknown and frequency-independent sheet surface resistivities in Ω/square. The identical dielectric spacers are represented by transmission lines, each with a delay time of $T = 1$ s, and a characteristic impedance $0 < Z_c < 1$, with $Z_c = 1/\sqrt{\epsilon_r}$, and with $1 < \epsilon_r < \infty$ being the relative dielectric constant of the spacers (which will be assumed known). The impedance normalization suggests that the network be embedded in a 1-Ω system, while the commensurate transmission lines make it convenient to utilize Richard's complex frequency surrogate $S = \Sigma + j\Omega = \tanh(s) = \tanh(\sigma + j\omega)$ to express the input properties [10]. For numerical calculations, a real valued frequency surrogate $f = 200\omega/\pi$ will be defined that automatically normalizes the absorber center frequency to $f = 100$. Bandwidth ($\mathcal{B}$) will be expressed in terms of these f-domain units throughout this paper and will therefore be in percentage units. Note that f should not be confused with the more conventional $f = \omega/(2\pi)$. Finally, only normal incidence will be considered, and to retain as much as possible of the underlying order in the pertinent analysis equations, the assumption will be made that a radome, typically with a different thickness and ϵ_r, is absent.

Manuscript received February 12, 1996; revised August 26, 1996.

The authors are with the Department of Electrical and Electronic Engineering, University of Stellenbosch, Stellenbosch 7599, South Africa.

Publisher Item Identifier S 0018-9480(96)08506-7.

II. Analysis Equations

It has been shown [2], [11] that the input impedance and reflection coefficient of the network in Fig. 1 can be expressed as

$$Z_{\text{in}}(S) = \frac{Z_c S P_N}{P_{N+1} - P_N}, \quad \text{and} \tag{1}$$

$$\rho(S) = \frac{(Z_c S + 1)P_N - P_{N+1}}{(Z_c S - 1)P_N + P_{N+1}} \tag{2}$$

with P_N and P_{N+1} the last two polynomials in the recursive set

$$P_{i+1} = (Z_c G_i S + 2)P_i + (S^2 - 1)P_{i-1} \tag{3}$$

with initial conditions $P_0 = 0, P_1 = 1$, and with $i = 1 \cdots N$. These equations are sufficient to expand Z_{in} and ρ in terms of Z_c and $G_{1 \cdots N}$ in general, although the number of terms and symbolic complexity both grow dramatically with increasing N. To circumvent this complexity during numerical synthesis, while retaining S as an independent variable, the coefficients of S in P_i may be derived recursively. Define

$$P_i(S) = \sum_{m=0}^{i-1} p_m^{(i)} S^m, \quad \text{for} \quad i = 1 \cdots N + 1 \tag{4}$$

where the superscript (i) does not denote any mathematical operation, but is simply used as convenient notation. To be mathematically complete, define $p_m^{(i)} \equiv 0$ for $m < 0$ and for $m \geq i$, which automatically includes the one initial condition, $P_0 = 0$. The second condition, $P_1 = 1$, and the recursive equation (3) for P_i, may now be implemented by defining the initial state as $p_{m=-2 \cdots N}^{(i=0 \cdots N+1)} = 0$, by setting $p_0^{(1)} = 1$, and finally by constructing a triangular set of coefficients by computing, for each $i = 2 \cdots N + 1$

$$p_m^{(i)} = Z_c G_{i-1} p_{m-1}^{(i-1)} + 2p_m^{(i-1)} + p_{m-2}^{(i-2)} - p_m^{(i-2)}, \quad \text{where} \quad m = 0 \cdots i - 1. \tag{5}$$

Note that this paper will present the reflection behavior (i.e., absorber performance) as the reflection coefficient magnitude expressed in dB, $\mathcal{A} = 20 \log_{10} |\rho|$, as a function of f.

III. Realizing Reflection Zeros

A. General Algorithm

It follows from (1)–(3) and the definition of S that the reflection zeros will be completely defined by the numerator of ρ alone. In fact, it is partially proved and hence postulated in [11] that such a given numerator is an overdetermined specification, with $N!$ conductance solutions in general. Luckily,

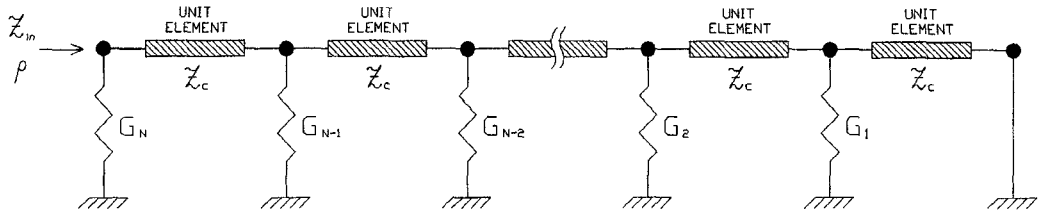

Fig. 1. The Jauman network model.

the two specific absorption behaviors that will be synthesized by controlling these zeros were found to be well-behaved and exhibited none, or only one, unique physical solution. (The uniqueness is a postulate.)

Let us now concentrate on realizing a given set of reflection zeros. First denote the numerator of ρ by $\mathcal{N}_\rho$ and express it as

$$\mathcal{N}_\rho(S) = -1 + \sum_{i=1}^{N} a_i S^i \tag{6}$$

with the a_i given by

$$a_i = Z_c p_{i-1}^{(N)} + p_i^{(N)} - p_i^{(N+1)} \tag{7}$$

for $i = 1 \cdots N$ and remembering $p_N^{(N)} \equiv 0$. For conciseness, introduce the matrix notation $\boldsymbol{a} = [a_1 \cdots a_N]^T$ and $\boldsymbol{G} = [G_1 \cdots G_N]^T$, where the superscript T indicates the transpose and where we have $\boldsymbol{a}$ computable from $\boldsymbol{G}$ through use of (5) and (7). This functional dependence of $\boldsymbol{a}$ on $\boldsymbol{G}$ may be approximated by assuming the linear relationship

$$\boldsymbol{a} \approx \overline{\boldsymbol{a}} + \overline{\boldsymbol{D}}(\boldsymbol{G} - \overline{\boldsymbol{G}}) \tag{8}$$

around the workpoint $\overline{\boldsymbol{G}}$. Notationwise we have $\boldsymbol{a}$ due to $\boldsymbol{G}$; $\overline{\boldsymbol{a}}$ due to $\overline{\boldsymbol{G}}$; $\boldsymbol{G}$ assumed to be in the vicinity of $\overline{\boldsymbol{G}}$; $\boldsymbol{a}, \overline{\boldsymbol{a}}, \boldsymbol{G}, \overline{\boldsymbol{G}}$ column vectors; and $\overline{\boldsymbol{D}}$ the (fortunately) square Jacobian matrix

$$\overline{\boldsymbol{D}} = [d_{ij}], \quad \text{with} \quad d_{ij} = \left.\frac{\partial a_i}{\partial G_j}\right|_{\overline{\boldsymbol{G}}} \tag{9}$$

with $i, j = 1 \cdots N$, and with all quantities real. It was found that finite difference approximations for the d_{ij} were not sufficiently accurate, or too slow, and that the more computationally efficient method given in the appendix, was needed. To complete the algorithm, rewrite the given $\mathcal{N}_\rho(S)$, which have to be realized as $-1 + \Sigma_{i=1}^{N} \hat{a}_i S^i$, enforce $\boldsymbol{a} = \hat{\boldsymbol{a}} = [\hat{a}_1, \cdots, \hat{a}_N]^T$ in (8) and denote intermediate solutions with superscripts to obtain the simple recursive improvement scheme

$$\boldsymbol{G}^{(i+1)} = \boldsymbol{G}^{(i)} + (\overline{\boldsymbol{D}}^{(i)})^{-1}(\hat{\boldsymbol{a}} - \boldsymbol{a}^{(i)}). \tag{10}$$

Given the reflection zero requirements $\hat{\boldsymbol{a}}$, an initial guess $\boldsymbol{G}^{(1)}$, and assuming stable convergence for the time being, (10) is simply applied until convergence, i.e., when the maximum difference between the elements of $\hat{\boldsymbol{a}}$ and $\boldsymbol{a}$ is sufficiently small (e.g. $\leq 10^{-9}$).

TABLE I
INTERMEDIATE RESULTS WHEN SYNTHESIZING THE $N = 3, \epsilon_r = 1$, BUTTERWORTH SOLUTION

i	$[G_1, G_2, G_3]$	$[a_1, a_2, a_3]$
1	[1.00000, 0.50000, 0.33333]	[0.0000, −1.5000, 0.0000]
2	[1.72581, 0.57258, 0.04301]	[−0.0000, 0.4109, 0.1768]
3	[1.64346, 0.51901, 0.10618]	[−0.0000, 0.0128, 0.0128]
4	[1.64404, 0.51427, 0.10914]	[−0.0000, 0.0000, 0.0000]
5	[1.64404, 0.51426, 0.10915]	[−0.0000, 0.0000, 0.0000]

B. Butterworth Synthesis

A Butterworth response may be obtained by realizing all N reflection zeros at $S \to \infty$, thereby yielding a maximally flat behavior around the center frequency where the reflection coefficient magnitude and its first $N-1$ derivatives with frequency, vanish. It has been shown [11] that this is equivalent to the specification $\mathcal{N}_\rho = -1$, i.e., $\hat{\boldsymbol{a}} = \boldsymbol{0}$. Next, it is postulated that for $\epsilon_r \leq \epsilon_{r,\max}(N)$, which is tabulated in [2], only one realizable solution for $\boldsymbol{G}$ exists and that it can be found by using $G_i^{(1)} = 1/i$ in (10).

As an illustration of the algorithm, consider the simple Butterworth synthesis, $N = 3$ and $\epsilon_r = 1$, of which the first five iterations are given in Table I. Also, to complement the discussion in [2], several practical solutions are given later, and to illustrate the severe spread in sheet resistivities mentioned in [2] it will be sufficient to state that we have, from the $N = 20, \epsilon_r = 1$ solution, that $R_1 \approx 0.5$ and $R_{20} > 5 \times 10^6$, with $R_{1\cdots 20}$ monotonic.

C. Equiripple Synthesis

If the reflection zeros are realized on the imaginary S-axis, at distinct and judiciously chosen (real) frequencies, rippled behaviors may be obtained with the maxima all at a specified level, $\mathcal{R}_{\text{dB}}$ expressed in dB. In Fig. 2 two such solutions for small N are depicted, and it is seen that in general, $M = \text{floor}(N/2)$ unique zeros might exist in the range $0 < f < 100$, not counting the necessary zero at $f = 100$ for N odd. The notation $\text{floor}(x)$ denotes the largest integer $\leq x$. Next, we number these zero positions with decreasing f, call them $z_{1\cdots M}$, and denote the spacings in between the z_i the lobe-widths $w_{1\cdots M}$. The following relationships exist:

$$N \text{ even:} \quad z_i = \begin{cases} 100 - \dfrac{w_1}{2} & i = 1 \\ z_{i-1} - w_i & i = 2 \cdots M, \end{cases} \quad \text{and} \tag{11}$$

$$N \text{ odd:} \quad z_i = \begin{cases} 100 - w_1 & i = 1 \\ z_{i-1} - w_i & i = 2 \cdots M. \end{cases} \tag{12}$$

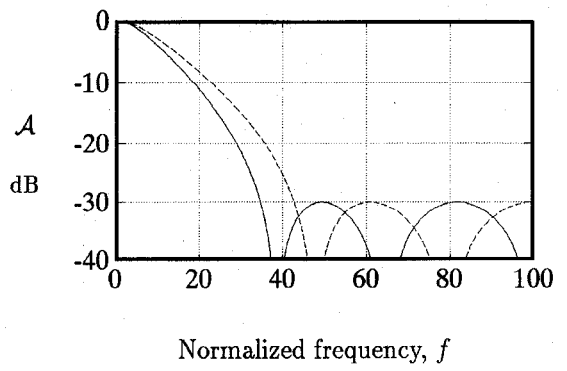

Fig. 2. Typical reflection behavior of Equiripple solutions. The dotted trace is for $N = 4$ and the solid trace for $N = 5$.

Next, associate a reflection maximum expressed in dB with each lobe, and denote them $m_{1\cdots M}$. As before, introduce the matrices $\boldsymbol{w} = [w_1, \cdots, w_M]^T, \boldsymbol{z} = [z_1, \cdots, z_M]^T$, and $\boldsymbol{m} = [m_1, \cdots, m_M]^T$. The algorithm now entails the repetitive execution of the following steps:

Step 1: Initially, and only during the first iteration, define the (almost) equispaced lobe-widths

$$w_1 = \frac{150}{N+0.5} \quad \text{for} \quad M = 1, \quad \text{and}$$
$$w_{1\cdots M-1} = \frac{200}{N+0.5}, \quad w_M = \frac{150}{N+0.5} \quad \text{for} \quad M > 1. \tag{13}$$

Step 2: This will be the entry point during iteration. From the current lobe-widths $\boldsymbol{w}$, find the zero positions with (11) or (12) and then construct

$$\mathcal{N}_\rho(S) = -\prod_{i=1}^{M} \left\{ \frac{S^2}{\tan^2(\pi z_i/200)} + 1 \right\}. \tag{14}$$

Note that $\mathcal{N}_\rho$ will of necessity always be an even polynomial in S, i.e., that $a_{2i-1} = 0$ for $i = 1 \cdots \text{floor}((N+1)/2)$, and that it will be of degree $2M$.

Step 3: To realize the constructed $\mathcal{N}_\rho$, simply apply the iterative algorithm given by (10), taking the current solution for $\boldsymbol{G}$, computed in Step 3 of the previous iteration, as $\boldsymbol{G}^{(1)}$. Should this be the first iteration, i.e., the realization of the zeros given by the initial lobe-widths (13), use $G_i^{(1)} = 1/i, i = 1 \cdots N$.

Step 4: With $\boldsymbol{G}$ known, $\boldsymbol{m}$ should now be computed. As will be made clear later on, the computation of $\boldsymbol{m}$ will also be needed in an inner loop, where partial derivatives will be approximated by finite differences. This necessitates the accurate computation of $\boldsymbol{m}$, which was implemented by evaluating $|\rho|$ at the zeros of its derivative with frequency. This derivative may be constructed in closed form, and its zeros may be found using a simple iterative procedure that starts at the midpoint of each lobe.

With $\boldsymbol{m}$ known, a test for convergence should take place that may be defined simply as when the maximum difference between any element of $\boldsymbol{m}$ and $\mathcal{R}_{\text{dB}}$ is sufficiently small (e.g., $\leq 10^{-4}$). Should this be the case, the synthesis is done and the frequency bandwidth may subsequently be computed. If not, the iteration proceeds to Step 5.

Step 5: This is the heart of the algorithm, where an unsatisfactory ripple behavior will be improved by judiciously perturbing the lobe-widths. This operation leans heavily on the fact that a reflection maximum in between two zeros (expressed in dB) is more or less proportional to its corresponding lobe-width (expressed in f-domain units). With this in mind, each maximum is now approximated by a linear combination of *all* the lobe-widths, i.e.,

$$\boldsymbol{m} \approx \overline{\boldsymbol{m}} + \overline{\boldsymbol{E}}(\boldsymbol{w} - \overline{\boldsymbol{w}}). \tag{15}$$

Notationwise, we have $\boldsymbol{m}$ due to $\boldsymbol{w}$; $\overline{\boldsymbol{m}}$ due to $\overline{\boldsymbol{w}}$ (the current maxima and lobe-widths); the new lobe-widths in $\boldsymbol{w}$ assumed to be in the vicinity of $\overline{\boldsymbol{w}}$; $\boldsymbol{m}, \overline{\boldsymbol{m}}, \boldsymbol{w}$, and $\overline{\boldsymbol{w}}$ column vectors; and $\overline{\boldsymbol{E}}$ the (again, fortunately) square Jacobian matrix

$$\overline{\boldsymbol{E}} = [e_{ij}] \quad \text{with} \quad e_{ij} = \left.\frac{\partial m_i}{\partial w_j}\right|_{\overline{\boldsymbol{w}}} \tag{16}$$

with $i, j = 1 \cdots M$. The partial derivatives in $\overline{\boldsymbol{E}}$ may be approximated by finite differences, in particular by perturbing the lobe widths one by one, each time retracing the complete cycle from Step 2 up to the recomputation of $\boldsymbol{m}$ and by observing the resulting changes in $\boldsymbol{m}$. Note that these perturbed intermediate quantities should only be used to build up $\overline{\boldsymbol{E}}$, and that they should be discarded afterwards. It was found that width perturbations of 0.001 f-domain units are sufficiently small for all reasonable $\mathcal{R}_{\text{dB}}$, and N up to at least 20. Note also from (11) and (12) that a width-perturbation in lobe j will cause shifts in *all* the remaining zero positions, namely $z_i, i = j \cdots M$, with small corresponding shifts in the positions of the corresponding maxima.

Solving (15) for $\boldsymbol{w}$ by enforcing $m_{1\cdots M} = \mathcal{R}_{\text{dB}}$ results in the following width-improvement matrix equation:

$$\boldsymbol{w} = \overline{\boldsymbol{w}} + \beta(\boldsymbol{\Delta w}), \quad \text{with} \tag{17}$$
$$\boldsymbol{\Delta w} = (\overline{\boldsymbol{E}})^{-1}(\mathcal{R}_{\text{dB}} - \overline{\boldsymbol{m}}) \tag{18}$$

which is *not* recursive. The meaning of $\mathcal{R}_{\text{dB}} - \overline{\boldsymbol{m}}$ is that each element of the vector $\overline{\boldsymbol{m}}$ should be subtracted from the scalar $\mathcal{R}_{\text{dB}}$, thereby again resulting in a vector. It is also important to note the damping constant $0 < \beta \leq 1$, which was implemented to subdue instabilities in the first few iterations of certain synthesis runs. Specifically, these occurred due to the rough assumption of linearity in (15), which induced large (and sometimes unrealizable) lobe-width improvements. These in turn translated to big changes in the coefficients of $\mathcal{N}_\rho(S)$, which could not be realized with (10).

This unstable behavior was controlled by restricting the maximum lobe-width change to be $25/(N+2)$-domain units. Particularly, β is derived from the proposed lobe-width improvements $\boldsymbol{\Delta w}$ given by (18), as

$$\beta = \min\left(1, \frac{25}{(N+2)\max\{|\Delta w_1|, \cdots, |\Delta w_M|\}}\right). \tag{19}$$

Note that final convergence is unaffected, as we then have $\beta = 1$. With (17) and (19) an improved set of lobe-widths may now be computed. These new widths should then be used in the next iteration, by injecting them into Step 2.

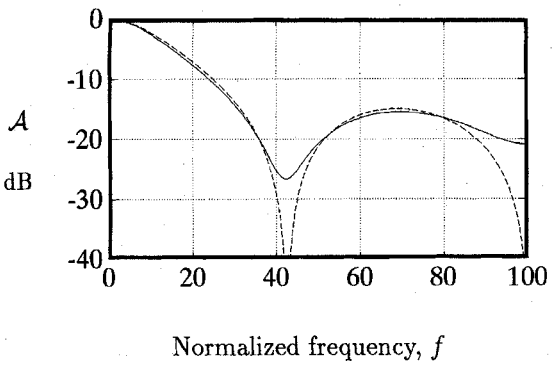

Fig. 3. Reflection behavior for the $N = 3, \epsilon_r = 1, \mathcal{R}_{\rm dB} = -15\,{\rm dB}$ Equiripple parent solution (dotted), and the Chebyshev solution optimized over the same ($f_c = 31.4519$) parent bandwidth (solid).

The first few iterations in the $N = 3, \epsilon_r = 1$ and $\mathcal{R}_{\rm dB} = -15\,{\rm dB}$ Equiripple synthesis are shown in Table II and clearly illustrate the algorithm. As another example, the $N = 20, \epsilon_r = 1$ and $\mathcal{R}_{\rm dB} = -20\,{\rm dB}$ solution has $3 < R_{1\ldots20} < 30$, which is seen to be much less of a spread than the corresponding Butterworth solution (see the comments in [2]). As in the Butterworth case, it is postulated that for $\epsilon_r \leq \epsilon_{r,\max}(N, \mathcal{R}_{\rm db})$, which is tabulated in [2], only one realizable solution for $\boldsymbol{G}$ exists, and that it can be found by using the algorithm as presented here. Lastly, a few solutions of practical interest are tabulated later.

IV. Optimal Chebyshev Synthesis

Experience gained during the development of the Equiripple synthesis algorithm indicated that such solutions are very close to local optimality. Numerical investigations, however, found small improvements in either the ripple level or the frequency bandwidth, and sometimes both. These potential improvements are negligible for practical purposes, but the nonoptimality of the Equiripple solutions was quite unexpected and felt to be important from a scientifically fundamental point of view.

The synthesis algorithm that was developed to find these optimal solutions will invoke Chebyshev's fundamental theorem and will thus be named in honor of him. The procedure is to assume a successful Equiripple synthesis, and then to reduce the reflection maxima (over the parent Equiripple solution's bandwidth) as much as possible. The algorithm will operate directly on the conductances, and its objectives will be the simultaneous reduction and ultimate vanishing of $M = \text{floor}(N/2)$ errors representing the differences between the maxima, and N errors indicative of the deviation from an optimal situation. Together, vanishing of these errors corresponds to a locally optimal situation, which will be heuristically conjectured to be global. All the pertinent numerical techniques that will be used have already been introduced, and the algorithm will thus be presented in a concise format.

As may be expected, the general structure of the rippled reflection coefficient magnitude does not change much when an Equiripple solution is optimized. This is shown in Fig. 3. Therefore, the same numbering scheme described earlier will be employed for the maxima, i.e., $m_{1\ldots M}$. As before, only the respective values in dB will be of interest, and not

TABLE II
Intermediate Results When Synthesizing the $N = 3, \epsilon_r = 1, \mathcal{R}_{\rm dB} = -15\,{\rm dB}$ Equiripple Solution

Equation	Results
(13)	Initialize : $w_1 = 42\frac{6}{7}$
(12)	$z_1 = 57\frac{1}{7}$
(14)	$\mathcal{N}_\rho = -0.6360S^2 - 1$, i.e. $\hat{\mathbf{a}} = [0, -0.6360, 0]^T$
(10), $i = 1$	$G_1 = 1.0000$, $G_2 = 0.50000$, $G_3 = 0.33333$
(10), $i = 2$	$G_1 = 1.4181$, $G_2 = 0.54181$, $G_3 = 0.16610$
(10), $i = 3$	$G_1 = 1.3896$, $G_2 = 0.51837$, $G_3 = 0.19121$
(10), $i = 4$	$G_1 = 1.3897$, $G_2 = 0.51759$, $G_3 = 0.19170$
See text	Convergence reached.
See Step 4	$m_1 = -26.623$ dB
(16)	$e_{1,1} = 0.792$
(18)	$\Delta w_1 = 14.68$
(19)	$\beta = 0.341$
(17)	We have $\bar{w}_1 = 42\frac{6}{7}$, therefore $w_1 = 47\frac{6}{7}$.
(12)	$z_1 = 52\frac{1}{7}$
(14)	$\mathcal{N}_\rho = -0.8739S^2 - 1$, i.e. $\hat{\mathbf{a}} = [0, -0.8739, 0]^T$
(10), $i = 1$	$G_1 = 1.3897$, $G_2 = 0.51759$, $G_3 = 0.19170$
(10), $i = 2$	$G_1 = 1.2898$, $G_2 = 0.51733$, $G_3 = 0.22528$
(10), $i = 3$	$G_1 = 1.2878$, $G_2 = 0.51626$, $G_3 = 0.22650$
See text	Convergence reached.
See Step 4	$m_1 = -22.719$ dB
(16)	$e_{1,1} = 0.775$
(18)	$\Delta w_1 = 9.963$
(19)	$\beta = 0.502$
(17)	We have $\bar{w}_1 = 47\frac{6}{7}$, therefore $w_1 = 52\frac{6}{7}$.
(12)	$z_1 = 47\frac{1}{7}$
(14)	$\mathcal{N}_\rho = -1.1969S^2 - 1$, i.e. $\hat{\mathbf{a}} = [0, -1.1969, 0]^T$
(10), $i = 1$	$G_1 = 1.2878$, $G_2 = 0.51626$, $G_3 = 0.22650$
(10), $i = 2$	$G_1 = 1.1468$, $G_2 = 0.51335$, $G_3 = 0.27556$
(10), $i = 3$	$G_1 = 1.1430$, $G_2 = 0.51099$, $G_3 = 0.27840$
See text	Convergence reached.
See Step 4	$m_1 = -18.819$ dB
(16)	$e_{1,1} = 0.792$
(18)	$\Delta w_1 = 4.820$
(19)	$\beta = 1$
(17)	We have $\bar{w}_1 = 52\frac{6}{7}$, therefore $w_1 = 57.677$.
Iteration 4 : $m_1 = -14.851$ dB.	
Iteration 5 : $m_1 = -14.999$ dB.	
Iteration 6 $\Rightarrow$ Final solution : $G_1 = 0.94645$, $G_2 = 0.49410$, $G_3 = 0.35512$, $\mathcal{B} = 137.096\%$.	

the frequency points where they occur. To complete the formulation, one additional maximum is of interest, namely $m_{M+1} = 20\log_{10}|\rho|$, evaluated at the frequency point which defines the bandwidth of the parent Equiripple solution, f_c. Except for the fact that $|\rho|$ will always be evaluated at f_c, m_{M+1} will be treated in exactly the same way as the other maxima.

Step 1: Assuming known conductances, the $M+1$ maxima may be computed as before (see Step 4 of the Equiripple algorithm). With these maxima known, M errors of the first kind will now be defined as

$$[\mathcal{E}_1, \cdots, \mathcal{E}_M]^T = m_{M+1} - [m_1, \cdots, m_M]^T \qquad (20)$$

with each element of the vector being subtracted from the scalar m_{M+1}. Since the optimization initiates with an Equiripple solution, it follows that these errors will start out being zero. During optimization the maxima will differ slightly, however, and they will only equalize again upon convergence.

Step 2: The next step is to define errors of the second kind, which will be indicative of the nonoptimality of the current

TABLE III
INTERMEDIATE RESULTS WHEN OPTIMIZING THE $N = 3, \epsilon_r = 1, \mathcal{R}_{\mathrm{dB}} = -15$ dB EQUIRIPPLE PARENT SOLUTION TOWARDS THE OPTIMAL CHEBYSHEV SOLUTION

Equation	Results
(20)	$\mathcal{E}_1 = 0$
(22)	$\mathbf{Q} = \begin{bmatrix} -9.7046 & -6.7886 & 15.2929 \\ 1.9935 & -1.8947 & -18.2545 \end{bmatrix}$
(29)	$\mathcal{E}_2 = -5.4158, \mathcal{E}_3 = -7.0777, \mathcal{E}_4 = -6.5785$
See Step 4	$\mathbf{G} = \begin{bmatrix} 1.12254 & 0.508687 & 0.433493 \end{bmatrix}^T$
(20)	$\mathcal{E}_1 = -0.2985$
(22)	$\mathbf{Q} = \begin{bmatrix} -7.2461 & -6.4480 & 16.8322 \\ 3.5083 & 3.7961 & -10.3095 \end{bmatrix}$
(29)	$\mathcal{E}_2 = -0.7815, \mathcal{E}_3 = -0.0212, \mathcal{E}_4 = -0.3446$
See Step 4	$\mathbf{G} = \begin{bmatrix} 1.19434 & 0.489375 & 0.443681 \end{bmatrix}^T$
(20)	$\mathcal{E}_1 = -0.0358$
(22)	$\mathbf{Q} = \begin{bmatrix} -6.4652 & -7.2319 & 17.6069 \\ 3.5384 & 3.9051 & -9.7378 \end{bmatrix}$
(29)	$\mathcal{E}_2 = -0.0224, \mathcal{E}_3 = -0.0780, \mathcal{E}_4 = -0.0403$
See Step 4	$\mathbf{G} = \begin{bmatrix} 1.19576 & 0.490890 & 0.443508 \end{bmatrix}^T$
(20)	$\mathcal{E}_1 = 0.00002$
(22)	$\mathbf{Q} = \begin{bmatrix} -6.4695 & -7.2087 & 17.6660 \\ 3.5394 & 3.9437 & -9.6656 \end{bmatrix}$
(29)	$\mathcal{E}_2 = -0.0002, \mathcal{E}_3 = -0.0004, \mathcal{E}_4 = -0.0002$
See Step 4	$\mathbf{G} = \begin{bmatrix} 1.19577 & 0.490892 & 0.443512 \end{bmatrix}^T$

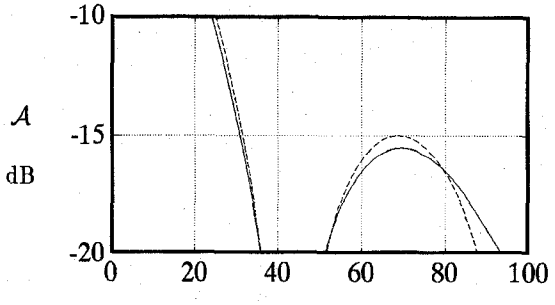

Fig. 4. Reflection behavior for the $N = 3, \epsilon_r = 1, \mathcal{R}_{\mathrm{dB}} = -15$ dB Equiripple parent solution (dotted) and the Chebyshev solution optimized over the same ($f_c = 31.4519$) parent bandwidth (solid). Note the exploded ordinate scale.

solution. Optimality in the present context simply implies that the $M + 1$ maxima under investigation must be at a state where they cannot all reduce simultaneously. To formalize this criterion, set up the following matrix equation:

$$\boldsymbol{Q\lambda} = [A_1, A_2, \cdots, A_{M+1}]^T, \quad \text{with} \tag{21}$$

$$\boldsymbol{Q} = [q_{ij}], \quad \text{where} \quad q_{ij} = \frac{\partial m_i}{\partial G_j}, \quad \text{and} \quad i = 1 \cdots M+1, \quad j = 1 \cdots N \tag{22}$$

with the A_i arbitrary nonzero real numbers with the same sign, with $\boldsymbol{\lambda} = [\lambda_1 \cdots \lambda_N]^T$ to be solved for, and with the q_{ij} approximated by finite differences. Because the q_{ij} will be nested in an outer loop (see Step 4), which will also approximate differentiation with respect to conductances by finite differences, these perturbations have to be chosen carefully, and it was found that conductance perturbations of $10^{-5}\mho$ were sufficiently small.

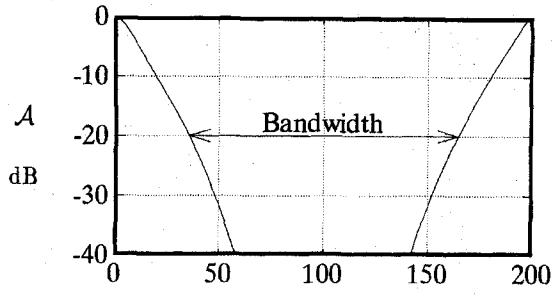

Fig. 5. Generic reflection behavior for the tabulated Butterworth solutions. Note the monotonic decrease from $f = 0$ to $f = 100$.

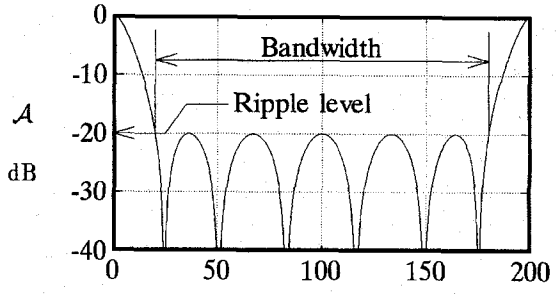

Fig. 6. Generic reflection behavior of the tabulated −20-dB Equiripple solutions. Note the N reflection zeros in the range $0 < f < 200$.

Optimality will have been reached when (21) has no solution [12], which explains the *no-solution* terminology often associated with this approach, and which is an expression of Chebyshev's fundamental theorem. It follows that (21) will have no possible solution for $\boldsymbol{\lambda}$ when the $M + 1$ rows of $\boldsymbol{Q}$ exhibit linear dependence, i.e., when $\alpha_{1 \cdots M+1}$, not all zero, exist such that

$$\sum_{i=1}^{M+1} \alpha_i q_{ij} = 0, \quad \text{for} \quad j = 1 \cdots N \tag{23}$$

with the signs of all the nonzero α_i the same and with all α_i real. It should be noted that the requirement on the signs of α_i was pointed out by Navot [13]. Although this sign requirement can not be enforced in the algorithm, it can be checked for and indeed was satisfied by all the examples worked out during the course of [11] and [2] and during the preparation of this paper.

Step 3: Now, since (23) will by necessity not be possible during optimization, N optimality errors may now be extracted from it. Stated loosely, these errors will be indicative of the "deviation from linear dependence in the rows of $\boldsymbol{Q}$." Without loss of generality, define $\alpha_{M+1} = -1$, keep in mind that all quantities are real, and restate (23) as follows:

$$\sum_{i=1}^{M} \alpha_i q_{ij} = q_{M+1,j} \quad \text{for} \quad j = 1 \cdots N. \tag{24}$$

Before proceeding, it will be convenient to segregate $\boldsymbol{Q}$ into

$$\boldsymbol{R} = [r_{ij}] \quad \text{with} \quad r_{ij} = q_{ji}, \quad \text{and} \quad i = 1 \cdots N, \quad j = 1 \cdots M \tag{25}$$

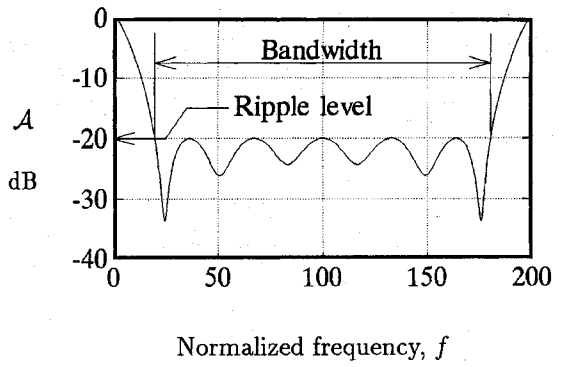

Fig. 7. Generic reflection behavior of the tabulated −20 dB Chebyshev solutions. Note the N reflection minima in the range $0 < f < 200$.

TABLE IV
NORMALIZED RESISTANCE (R_i) VALUES FOR BUTTERWORTH REFLECTION BEHAVIORS, WITH THE CORRESPONDING BANDWIDTHS COMPUTED AT THE $\mathcal{A} = -20$ dB LEVEL

N	$\epsilon_r = 1$	$\epsilon_r = 1.03$	$\epsilon_r = 1.1$
1	$R_1 = 1.00000$ $B = 25.26\%$	$R_1 = 1.00000$ $B = 24.90\%$	$R_1 = 1.00000$ $B = 24.11\%$
2	$R_1 = 0.707107$ $R_2 = 3.41421$ $B = 67.32\%$	$R_1 = 0.696733$ $R_2 = 3.54152$ $B = 66.79\%$	$R_1 = 0.674200$ $R_2 = 3.87027$ $B = 65.65\%$
3	$R_1 = 0.608257$ $R_2 = 1.94454$ $R_3 = 9.16207$ $B = 92.64\%$	$R_1 = 0.599334$ $R_2 = 1.91601$ $R_3 = 10.4295$ $B = 92.13\%$	$R_1 = 0.579950$ $R_2 = 1.85404$ $R_3 = 15.2290$ $B = 91.01\%$
4	$R_1 = 0.561038$ $R_2 = 1.49364$ $R_3 = 4.27818$ $R_4 = 22.5545$ $B = 108.92\%$	$R_1 = 0.552807$ $R_2 = 1.47173$ $R_3 = 4.21541$ $R_4 = 33.2137$ $B = 108.45\%$	NO SOLUTION
5	$R_1 = 0.535357$ $R_2 = 1.28591$ $R_3 = 2.91767$ $R_4 = 8.79951$ $R_5 = 53.1999$ $B = 120.31\%$	$R_1 = 0.527503$ $R_2 = 1.26705$ $R_3 = 2.87487$ $R_4 = 8.67041$ $R_5 = 238.792$ $B = 119.88\%$	NO SOLUTION
6	$R_1 = 0.520602$ $R_2 = 1.17288$ $R_3 = 2.32379$ $R_4 = 5.32786$ $R_5 = 17.6607$ $R_6 = 122.301$ $B = 128.78\%$	NO SOLUTION	NO SOLUTION
7	$R_1 = 0.511953$ $R_2 = 1.10625$ $R_3 = 2.00829$ $R_4 = 3.90673$ $R_5 = 9.52448$ $R_6 = 35.1300$ $R_7 = 276.238$ $B = 135.36\%$	NO SOLUTION	NO SOLUTION
8	$R_1 = 0.506871$ $R_2 = 1.06546$ $R_3 = 1.82256$ $R_4 = 3.18060$ $R_5 = 6.41672$ $R_6 = 16.9650$ $R_7 = 69.6897$ $R_8 = 615.734$ $B = 140.66\%$	NO SOLUTION	NO SOLUTION

and into

$$\boldsymbol{t} = [q_{M+1,1}, q_{M+1,2}, \cdots, q_{M+1,N}]^T. \tag{26}$$

This segregation, together with $\boldsymbol{\alpha} = [\alpha_1 \cdots \alpha_M]^T$, transforms (24) into

$$\boldsymbol{R\alpha} = \boldsymbol{t}. \tag{27}$$

It readily follows that (27) represents N linear equations in M unknowns, with $N > M$, that it will be overdetermined and also inconsistent in general. One way to find the "best" solution is to solve it in a minimum RMS sense [14, p. 143]

$$\alpha_* = (\boldsymbol{R}^T\boldsymbol{R})^{-1}\boldsymbol{R}^T\boldsymbol{t}. \tag{28}$$

This solution should now be subjected to the aforementioned sign-test. If successful, it may then be used in (27) to obtain N criteria, or errors, representing the "deviation from linear dependence" in $\boldsymbol{Q}$. In particular

$$[\mathcal{E}_{M+1} \cdots \mathcal{E}_{M+N}]^T = \boldsymbol{t} - \boldsymbol{R\alpha}_* = (1 - \boldsymbol{R}(\boldsymbol{R}^T\boldsymbol{R})^{-1}\boldsymbol{R}^T)\boldsymbol{t}. \tag{29}$$

Step 4: The last step is to group both kinds of errors together in $\boldsymbol{\mathcal{E}} = [\mathcal{E}_1 \cdots \mathcal{E}_{M+N}]^T$. If they are sufficiently small (e.g., $\max\{|\mathcal{E}_1|, |\mathcal{E}_2|, \cdots, |\mathcal{E}_{M+N}|\} \leq 10^{-6}$), the algorithm terminates and the synthesis is done. If not, the next step is to find an improved set of conductances $G_{1\cdots N}$, which will result in smaller errors. This may be done by approximating the functional dependence of $\boldsymbol{\mathcal{E}}$ on $\boldsymbol{G}$ as being linear; by approximating the partial derivatives by finite differences (using conductance perturbations of $10^{-4}\mho$) and by enforcing $\boldsymbol{\mathcal{E}} = 0$. This results in $M + N$ linear equations in the N unknown conductance improvements, which are also overdetermined and inconsistent in general. Again using the minimum RMS sense solution method, improved conductances may now be solved for and the algorithm then repeats from Step 1.

The algorithm was applied to the Equiripple parent solution of Table II, which had $f_c = 31.4519$. The results of the first four iterations are shown in Table III, and the final solution showed a 0.528 dB reduction in the ripple level. Both

TABLE V
NORMALIZED RESISTANCE (R_i) VALUES FOR $\mathcal{R}_{\text{dB}} = -20$ dB EQUIRIPPLE REFLECTION BEHAVIORS

N	$\epsilon_r = 1$	$\epsilon_r = 1.03$	$\epsilon_r = 1.1$
2	$R_1 = 0.826894$ $R_2 = 2.52955$ $B = 86.40\%$	$R_1 = 0.812910$ $R_2 = 2.59791$ $B = 85.88\%$	$R_1 = 0.782734$ $R_2 = 2.76845$ $B = 84.74\%$
3	$R_1 = 0.838716$ $R_2 = 1.94817$ $R_3 = 3.84076$ $B = 120.69\%$	$R_1 = 0.823232$ $R_2 = 1.91887$ $R_3 = 4.03772$ $B = 120.28\%$	$R_1 = 0.789942$ $R_2 = 1.85534$ $R_3 = 4.57236$ $B = 119.36\%$
4	$R_1 = 0.896298$ $R_2 = 1.75683$ $R_3 = 3.28899$ $R_4 = 4.79759$ $B = 139.71\%$	$R_1 = 0.878576$ $R_2 = 1.72844$ $R_3 = 3.24334$ $R_4 = 5.13014$ $B = 139.38\%$	$R_1 = 0.840582$ $R_2 = 1.66706$ $R_3 = 3.14417$ $R_4 = 6.09308$ $B = 138.66\%$
5	$R_1 = 0.975877$ $R_2 = 1.70002$ $R_3 = 2.86558$ $R_4 = 4.74914$ $R_5 = 5.49659$ $B = 151.49\%$	$R_1 = 0.955448$ $R_2 = 1.67112$ $R_3 = 2.82228$ $R_4 = 4.68707$ $R_5 = 5.95104$ $B = 151.23\%$	$R_1 = 0.911745$ $R_2 = 1.60881$ $R_3 = 2.72846$ $R_4 = 4.55211$ $R_5 = 7.33340$ $B = 150.64\%$
6	$R_1 = 1.07070$ $R_2 = 1.69661$ $R_3 = 2.68251$ $R_4 = 4.09579$ $R_5 = 6.28190$ $R_6 = 6.02222$ $B = 159.46\%$	$R_1 = 1.04720$ $R_2 = 1.66647$ $R_3 = 2.63988$ $R_4 = 4.03689$ $R_5 = 6.20351$ $R_6 = 6.58139$ $B = 159.23\%$	$R_1 = 0.997001$ $R_2 = 1.60160$ $R_3 = 2.54771$ $R_4 = 3.90910$ $R_5 = 6.03294$ $R_6 = 8.34865$ $B = 158.74\%$
7	$R_1 = 1.17776$ $R_2 = 1.72238$ $R_3 = 2.59707$ $R_4 = 3.77571$ $R_5 = 5.41532$ $R_6 = 7.86210$ $R_7 = 6.42951$ $B = 165.19\%$	$R_1 = 1.15088$ $R_2 = 1.69048$ $R_3 = 2.55420$ $R_4 = 3.71836$ $R_5 = 5.34048$ $R_6 = 7.76747$ $R_7 = 7.07770$ $B = 164.99\%$	$R_1 = 1.09355$ $R_2 = 1.62195$ $R_3 = 2.46164$ $R_4 = 3.59416$ $R_5 = 5.17798$ $R_6 = 7.56150$ $R_7 = 9.18968$ $B = 164.57\%$
8	$R_1 = 1.29513$ $R_2 = 1.76763$ $R_3 = 2.56200$ $R_4 = 3.59991$ $R_5 = 4.95560$ $R_6 = 6.80274$ $R_7 = 9.47503$ $R_8 = 6.75346$ $B = 169.50\%$	$R_1 = 1.26464$ $R_2 = 1.73356$ $R_3 = 2.51829$ $R_4 = 3.54310$ $R_5 = 4.88296$ $R_6 = 6.71179$ $R_7 = 9.36425$ $R_8 = 7.47744$ $B = 169.33\%$	$R_1 = 1.19966$ $R_2 = 1.66053$ $R_3 = 2.42405$ $R_4 = 3.42022$ $R_5 = 4.72550$ $R_6 = 6.51419$ $R_7 = 9.12304$ $R_8 = 9.89563$ $B = 168.96\%$

TABLE VI
NORMALIZED RESISTANCE (R_i) VALUES FOR $\mathcal{R}_{dB} = -20$ dB CHEBYSHEV REFLECTION BEHAVIORS (SEE TEXT)

N	$\epsilon_r = 1$	$\epsilon_r = 1.03$	$\epsilon_r = 1.1$
2	$R_1 = 0.790001$ $R_2 = 2.31363$ $\mathcal{B} = 87.18\%$	$R_1 = 0.777107$ $R_2 = 2.37078$ $\mathcal{B} = 86\ 65\%$	$R_1 = 0.749242$ $R_2 = 2.51221$ $\mathcal{B} = 85\ 48\%$
3	$R_1 = 0.760552$ $R_2 = 1.90474$ $R_3 = 3.23075$ $\mathcal{B} = 121.77\%$	$R_1 = 0.747693$ $R_2 = 1.87516$ $R_3 = 3.36944$ $\mathcal{B} = 121\ 35\%$	$R_1 = 0.719913$ $R_2 = 1.81124$ $R_3 = 3.73492$ $\mathcal{B} = 120.41\%$
4	$R_1 = 0.767007$ $R_2 = 1\ 68882$ $R_3 = 3.23865$ $R_4 = 3.77565$ $\mathcal{B} = 140.83\%$	$R_1 = 0.753815$ $R_2 = 1.66163$ $R_3 = 3.18990$ $R_4 = 3.97977$ $\mathcal{B} = 140.50\%$	$R_1 = 0.725313$ $R_2 = 1.60287$ $R_3 = 3.08463$ $R_4 = 4\ 53916$ $\mathcal{B} = 139.76\%$
5	$R_1 = 0\ 781686$ $R_2 = 1.61910$ $R_3 = 2.75740$ $R_4 = 4.75326$ $R_5 = 4\ 10571$ $\mathcal{B} = 152\ 57\%$	$R_1 = 0.768171$ $R_2 = 1.59221$ $R_3 = 2.71489$ $R_4 = 4.68207$ $R_5 = 4\ 35601$ $\mathcal{B} = 152.30\%$	$R_1 = 0.738956$ $R_2 = 1\ 53415$ $R_3 = 2\ 62296$ $R_4 = 4.52863$ $R_5 = 5\ 05893$ $\mathcal{B} = 151.70\%$
6	$R_1 = 0.797876$ $R_2 = 1.59606$ $R_3 = 2\ 57263$ $R_4 = 3.94280$ $R_5 = 6.44053$ $R_6 = 4.31436$ $\mathcal{B} = 160.46\%$	$R_1 = 0.784103$ $R_2 = 1.56898$ $R_3 = 2\ 53161$ $R_4 = 3.88375$ $R_5 = 6.34292$ $R_6 = 4.59655$ $\mathcal{B} = 160.24\%$	$R_1 = 0.754312$ $R_2 = 1.51053$ $R_3 = 2.44296$ $R_4 = 3.75606$ $R_5 = 6.13296$ $R_6 = 5.40178$ $\mathcal{B} = 159\ 73\%$
7	$R_1 = 0\ 813430$ $R_2 = 1.59356$ $R_3 = 2.48273$ $R_4 = 3\ 62175$ $R_5 = 5.22681$ $R_6 = 8\ 30589$ $R_7 = 4\ 45160$ $\mathcal{B} = 166\ 12\%$	$R_1 = 0\ 799464$ $R_2 = 1\ 56612$ $R_3 = 2\ 44214$ $R_4 = 3.56575$ $R_5 = 5.14991$ $R_6 = 8.17724$ $R_7 = 4.75604$ $\mathcal{B} = 165.92\%$	$R_1 = 0.769238$ $R_2 = 1.50689$ $R_3 = 2.35445$ $R_4 = 3.44465$ $R_5 = 4.98371$ $R_6 = 7\ 90105$ $R_7 = 5\ 63413$ $\mathcal{B} = 165\ 49\%$
8	$R_1 = 0.827640$ $R_2 = 1\ 60137$ $R_3 = 2.43715$ $R_4 = 3.44990$ $R_5 = 4.75290$ $R_6 = 6\ 59900$ $R_7 = 10.3609$ $R_8 = 4.54487$ $\mathcal{B} = 170.36\%$	$R_1 = 0.813537$ $R_2 = 1\ 57351$ $R_3 = 2.39653$ $R_4 = 3.39514$ $R_5 = 4.68106$ $R_6 = 6.50282$ $R_7 = 10\ 1959$ $R_8 = 4.86507$ $\mathcal{B} = 170.19\%$	$R_1 = 0.782994$ $R_2 = 1.51338$ $R_3 = 2\ 30882$ $R_4 = 3\ 27678$ $R_5 = 4.52569$ $R_6 = 6\ 29508$ $R_7 = 9.84235$ $R_8 = 5.79556$ $\mathcal{B} = 169.81\%$

responses are shown in Fig. 3, with the region of interest enlarged in Fig. 4.

V. NUMERICAL RESULTS

Numerical results of a practical nature are shown in Figs. 5–7 and Tables IV–VI. Note that the abscissa now extends to $f = 200$ to be consistent with the format adopted by most of the literature on Jauman absorbers. Of special interest are the -20 dB Chebyshev solutions. It has been stated that the algorithm is designed to *improve* on a given Equiripple solution, with the potential ripple level improvement not known *a priori*. To generate the solutions in Table VI, a small modification was therefore needed. Specifically, after optimizing the -20 dB Equiripple solutions, the cutoff frequency f_c was decreased by small amounts (i.e., small bandwidth increases), and the algorithm was applied repetitively until the ripple level returned back to -20 dB.

VI. CONCLUSION

The electric screen Jauman Absorber has a very structured topology, and consequently it may be represented by a simple equivalent circuit. The three synthesis algorithms introduced in [2] and presented here in detail augment the surprisingly sparse collection of absorber synthesis techniques that could be found in the open literature. Although these algorithms are iterative in nature, they are robust, tractable, and rigorous, and synthesize two classical solutions (Butterworth and Equiripple responses) and also the optimal bandwidth response (named in honor of Chebyshev). Illustrative results are given in lookup tables, and although normal incidence and the absence of a radome are implicitly assumed, these results may aid in practical Jauman Absorber design.

APPENDIX
THE COMPUTATION OF d_{ij}

First define intermediate derivatives

$$X_{j,i,m} = \frac{\partial p_m^{(i)}}{\partial G_j} \tag{30}$$

evaluated implicitly around $\overline{G}$. Next, use (5) to construct the recursive relation

$$\begin{aligned} X_{j,i,m} = {} & Z_c\{G_{i-1}X_{j,i-1,m-1} + p_{m-1}^{(i-1)}\delta(i-j-1)\} \\ & + 2X_{j,i-1,m} + X_{j,i-2,m-2} - X_{j,i-2,m} \end{aligned} \tag{31}$$

with $\delta(0) = 1, \delta(i \neq 0) = 0$, and where the ranges of j, i, and m have to be carefully selected to accommodate all the initial and edge conditions. Specifically, to construct the N triangular sets of X's, perform the following steps:

```
For j = 1 ··· N do
  Initialize: X_{j,i=0···N+1,m=−1···N} = 0.
  If j = 1, set X_{j=1,2,1} = Z_c.
  For i = max(3, j + 1) ··· N + 1 do
    For m = 1 ··· i − 1 do
      Use (31) to compute X_{j,i,m}.
    Next m.
  Next i.
Next j.
```
(32)

Finally, use (7) to construct

$$d_{ij} = \frac{\partial a_i}{\partial G_j} = Z_c X_{j,N,i-1} + X_{j,N,i} - X_{j,N+1,i} \tag{33}$$

with $i, j = 1 \cdots N$.

ACKNOWLEDGMENT

Prof. I. Navot, from the Technion-Israel Institute of Technology, Haifa, worked on the Jauman absorber problem during several visits to the University of Stellenbosch and his technical inputs and suggestions were very helpful. In particular, he suggested investigating the no-solution technique to obtain the Chebyshev solutions.

REFERENCES

[1] W. H. Emerson, "Electromagnetic wave absorbers and anechoic chambers through the years," *IEEE Trans. Antennas Propagat.*, vol. AP-21, no. 4, pp. 484–490, July 1973.
[2] L. J. du Toit, "The design of Jauman absorbers," *IEEE Antennas Propagat. Mag.*, vol. 36, no. 6, pp. 17–25, Dec. 1994.
[3] P. T. C. Wong, B. Chambers, A. P. Anderson, and P. V. Wright, "Large area conducting polymer composites and their use in microwave absorbing material," *Electron. Lett.*, vol. 28, no. 17, pp. 1651–1653, Aug. 13, 1992.
[4] B Chambers, "Optimum design of a Salisbury screen radar absorber," *Electron. Lett.*, vol. 30, no. 16, pp. 1353–1354, Aug. 4, 1994.
[5] ——, "Frequency tuning characteristics of capacitively loaded Salisbury screen radar absorber," *Electron. Lett.*, vol. 30, no. 19, pp. 1626–1628, Sept. 15, 1994.

[6] B. Chambers and A. Tennant, "Design of wideband Jaumann radar absorbers with optimum oblique incidence performance," *Electron. Lett.*, vol. 30, no. 18, pp. 1530–1532, Sept. 1, 1994.
[7] A. Tennant and B. Chambers, "Adaptive optimization techniques for the design of microwave absorbers," in *Conf. Adaptive Computing in Engineering Design and Control*, Univ. of Plymouth, U.K., Sept. 21–22, 1994.
[8] B. Chambers and A. Tennant, "Characteristics of Jaumann radar absorbers," in *Microwaves 94 Conf.*, London, U.K., Oct. 25–27, 1994.
[9] E. F. Knott and C. D. Lunden, "The two-sheet capacitive Jaumann absorber," *IEEE Trans. Antennas Propagat.*, vol. 43, no. 11, pp. 1339–1343, Nov. 1995.
[10] P. I. Richards, "Resistor-transmission-line circuits," *Proc. IRE,* vol. 36, pp. 217–220, Feb. 1948.
[11] L. J. du Toit, "Analysis and Synthesis Algorithms for the Electric Screen Jauman Electromagnetic Wave Absorber," Ph.D. dissertation, Univ. of Stellenbosch, Stellenbosch, South Africa, 1993.
[12] P. R. Clement, "The Chebyshev approximation method," *Quarterly App. Math.*, vol. 11, no. 2, pp. 167–183, July 1953.
[13] I. Navot, Dept. of Electrical Engineering, Technion, Haifa, Israel, Private communication during his examination of [11], 1993.
[14] B. Noble, *Applied Linear Algebra.* Englewood Cliffs, NJ: Prentice Hall, 1969.

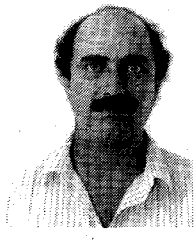

Leendert Johannes du Toit (M'92) was born in Bellville, South Africa, in 1963. He received the Bachelor and Master degrees in electronic engineering in 1985 and 1987, respectively, from the University of Stellenbosch, Stellenbosch, South Africa. In 1993, he received the Doctoral degree from the same university for research on microwave absorbing materials in general and the Jauman absorber in particular.

He was a Research Assistant at the University of Stellenbosch while working toward the Ph.D. degree, and in July 1991, was appointed as a Design Engineer, Radar Division, Reutech Systems, Stellenbosch. He is currently interested in microwave antenna design, specifically in large planar arrays and the associated passive components.

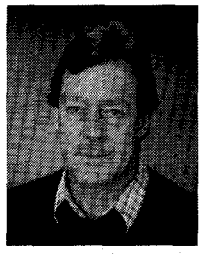

Johannes Hendrik Cloete (M'77) was born in Clocolan, Orange Free State, South Africa, in 1945. He received the B.Sc., B.Eng., and Ph.D. (Eng) degrees in electrical engineering from the University of Stellenbosch, Stellenbosch, South Africa, and the M.S. degree in electrical engineering from the University of California, Berkeley.

He has been a Professor, Department of Electrical and Electronic Engineering, University of Stellenbosch, since 1984. His research interests are the electromagnetic properties of materials, experimental and analytical methods for characterizing them, and antenna engineering.